

Supporting Information

Electrosynthesis of Nitrate via the Oxidation of Nitrogen

Anyong Chen, ^{*a} Guangyue Wang, ^a Yihui Tian, ^c Zuochao Wang, ^{*b, c} Hongdong Li, ^{*c} and Hailin Cong^{*a}

^a College of Chemistry Chemical Engineering and Materials Science, Zaozhuang University, Zaozhuang 277160, China.

^b State Key Laboratory of Catalysis, Collaborative Innovation Center of Chemistry for Energy Materials (iChEM), Dalian Institute of Chemical Physics, Chinese Academy of Science, Zhongshan Road 457, Dalian 116023, China

^c State Key Laboratory Base of Eco-Chemical Engineering, Ministry of Education, International Science and Technology Cooperation Base of Eco-Chemical Engineering and Green Manufacturing, College of Chemistry and Molecular Engineering, Qingdao University of Science and Technology, Qingdao 266042, P. R. China

E-mail: chenanyong@uzz.edu.cn

Experimental Section

Chemicals

Cobalt acetate ($(\text{CH}_3\text{COO})_2\text{Co}$ 98%) was purchased from Shanghai Macklin Biochemical Technology Co., Ltd, China. Sodium citrate dihydrate ($\text{C}_6\text{H}_5\text{Na}_3\text{-O}_7\cdot 2\text{H}_2\text{O}$, 99%), Sodium fluoride ($\text{K}_3[\text{Co}(\text{CN})_6]$, 99%), Sodium sulfate ($\text{Na}_2\text{SO}_4\cdot\text{H}_2\text{O}$, 99%), Sodium tetrachloropalladate (II) (Na_2PdCl_4 , 98%) were purchased from Shanghai Aladdin Biochemical Technology Co., Ltd, China. Nafion solution (5%) was purchased from Sigma Aldrich. Ethanol ($\text{C}_2\text{H}_5\text{OH}$) was purchased from Sinopharm Chemical Reagent Co., Ltd. Ultrapure water (Millipore Milli-Q grade) with a resistivity of 18.2 $\text{M}\Omega$ was used in all the experiments.

Synthesis of Co-Co Prussian blue analogues (PBA) nanocubes

In a typical synthesis, 0.6 mmol of cobalt acetate and 0.9 mmol of sodium citrate were dissolved in 20 mL of deionized (DI) water to form solution A. At the same time, 0.4 mmol of potassium hexacyanocobaltate (III) was dissolved in 20 mL of DI water to form solution B. Then, solutions A and B were mixed together under magnetic stirring for 1 min. The obtained mixed solution was aged for 12 h at room temperature. Then, the obtained black gelatinous solutions were collected by centrifugation at 8000 rpm for 3 min, and washed 3 times with DI and ethanol. Finally, the precipitates were dried at 70 °C overnight.

Synthesis of $\text{PdO}_x\text{-Co}_3\text{O}_4$ nanoboxes

For the synthesis of Pd/PBA nanocubes: 10 mg of sodium tetrachloropalladate(II) was dissolved in 2 mL of DI water. At the same time, 50 mg of PBA was dissolved in 8 mL of methanol (MeOH) at ambient temperature. Then, the sodium tetrachloropalladate (II) solution was slowly poured into the PBA solution under magnetic stirring for 5 min, and the mixed solution was aged at 90 °C for 1 h. Subsequently, the suspended solid was cooled to room temperature and collected through washing with ethanol and deionized water three times, and drying at 60 °C for 12 h.

Synthesis of the $\text{PdO}_x\text{-Co}_3\text{O}_4$ nanoboxes: In a typical synthesis, the as-prepared Pd/PBA nanocubes were annealed at 350 °C for 2 h with a heating temperature rate of 2 °C min^{-1} in air.

Characterization

The scanning electron microscopy (SEM) images were acquired from a Hitachi S-4800 scanning electron microscope. Transmission electron microscope (TEM) and high-resolution transmission electron microscope images were taken using a JEOL-2100F system. The X-ray diffraction (XRD) was measured using a Bruker D8 Focus Diffraction System with a Cu $\text{K}\alpha$ source ($\lambda = 0.154178$ nm). X-ray photoelectron spectrum analysis was recorded via a PHI 5000 Versaprobe system using monochromatic Al $\text{K}\alpha$ radiation. All binding energies were revised according to the C1s peak at 284.8 eV. The ultraviolet-visible (UV-Vis) absorbance spectra were measured on a Beijing Purkinje General T6 new century spectrophotometer. Anion

chromatography was performed on an ICS-1100, Thermo. The concentration of ^{15}N isotope labeling was established by isotopic mass spectrometry (MAT-271). The pH values of the electrolytes were determined using a pH-meter (LE438pH electrode, Mettler Toledo, USA).

Ion-concentration detection methods

The electrolytes pre and post test were first diluted to appropriate concentration and then tested using a UV-Vis spectrophotometer to quantify the concentration. The concentrations of nitrate-N, nitrite-N and ammonia-N were estimated by UV-Vis spectrophotometry according to the standard method. The specific approaches are as follows.

Determination of nitrate-N

First, a certain amount of electrolyte was taken out of the electrolytic cell and diluted to 5 mL to the detection range. Then, 0.1 mL 1 M HCl and 0.01 mL 0.8 wt% sulfamic acid solution were added to the aforementioned solution. The absorption spectrum was tested using an ultraviolet-visible spectrophotometer and the absorption intensities at wavelengths of 220 and 275 nm were recorded. The final absorbance value was calculated using the equation: $A = A_{220\text{nm}} - 2A_{275\text{nm}}$. The concentration-absorbance curve was made using a series of standard potassium nitrate solutions and the potassium nitrate crystal was dried at 105–110 °C for 2 h in advance.

Determination of nitrite-N

A mixture of p-aminobenzenesulfonamide (4 g), N-(1-Naphthyl)ethylenediamine dihydrochloride (0.2 g), ultrapure water (50 mL) and phosphoric acid (10 mL, $\rho = 1.70 \text{ g mL}^{-1}$) was used as a color reagent. A certain amount of electrolyte was taken from the electrolytic cell and diluted to 5 mL to the detection range. Next, 0.1 mL color reagent was added into the aforementioned 5-mL solution and mixed to uniformity, and the absorption intensity at a wavelength of 540 nm was recorded after sitting for 20 min. The concentration absorbance curve was calibrated using a series of standard sodium nitrite solutions.

Electrochemical tests

Typically, 5 mg of electrocatalyst and 100 μL of 5 wt.% Nafion solution were dispersed in 1 mL of ethanol by sonicating for 1 h to form a homogenous ink. Then the as-prepared ink was loaded onto a carbon paper within an area of $1 \times 1 \text{ cm}^2$ and dried under vacuum condition overnight. All electrochemical NOR tests were carried out at room temperature in a gas-tight two compartment H-type cell, which was separated by a Nafion 117 membrane (DuPont). To evaluate the electrocatalytic NOR activity of $\text{PdO}_x\text{-Co}_3\text{O}_4$ NBs under ambient conditions, the NOR electrochemical tests were performed in 0.1 M Na_2SO_4 solution with a three-electrode system. Before the tests, the N_2 or Ar was inflated into the electrolyte for 30 min, and the current densities varying with time at different potentials (1.5 V to 1.9 V vs. RHE) were observed for 10 hours.

Note that Nafion membrane is impermeable to anions. Before the tests, the Nafion membrane was pre-treated in 3% H_2O_2 solution and 5% H_2SO_4 solution as well as ultra-pure water in sequence. The high-purity

N₂ (99.9995%) and Ar (99.9995%) gas were prepurified by passage through an acidic solution and a silica gel sorbent tube to remove any possible sources of N contamination (e.g. ammonia), and subsequently bubbled through the electrolyte for at least half hour before NOR tests. The gas flow rate was fixed at 10 mL min⁻¹. Linear sweep voltammogram (LSV) was performed in a 0.1 M Na₂SO₄ solution at a scan rate of 5 mV s⁻¹. For NOR experiments, potentiostatic tests were conducted in the N₂-saturated 0.1 M Na₂SO₄ electrolyte (10 mL) with continuous N₂ feeding. The electrolytic cell needs to be reprocessed to remove the contaminants attached to the surface after each cycle test. For the electrochemical impedance (EIS) measurements, the frequency was swept in a range of 10⁶-0.01 Hz with a perturbation alternating current amplitude of 10 mV at open circuit condition. Furthermore, the concentration of produced nitrate was systematically detected and quantified by ion chromatography (930 compact IC Flex, Metrohm). Additionally, for ¹⁵N₂ isotope (Sigma-Aldrich, 98 atom % ¹⁵N) labelling experiment, after 50 h of NOR with ¹⁵N₂ feeding gas, the obtained ¹⁵NO₃⁻ containing electrolyte was analyzed by ¹⁵N nuclear magnetic resonance (NMR, JEOL ECA400). Note that the test electrolytes were subjected to the concentration treatment (to 0.5 mL) before both IC and NMR analysis.

The yield rate of nitrate production was calculated by the following equation:

$$r_{NO_3^-} = (C \times V) / (t \times m) \quad \text{Equation S1}$$

where C is the measured nitrate molar concentration, V is the volume of the electrolyte, t is the electrochemical oxidation reaction time, and m is the loading mass of the electrocatalysts.

The Faradaic efficiency of nitrate formation can be calculated as follow:

$$FE_{NO_3^-} = (5F \times C \times V) / Q \quad \text{Equation S2}$$

where F is the Faraday constant, C is the measured nitrate concentration, V is the volume of the electrolyte, and Q is the total charge passed through the electrode in the electrocatalytic process.

The selection of neutral solutions for electrochemical NOR mainly due to the consideration to avoid strong OER during the whole oxidation kinetics. According to Partial Pourbaix diagram for the N₂-H₂O system, acidic solution is not thermodynamically favorable for NOR. While for alkaline solution, the extensive OH⁻ will preferentially occupy the active center of our catalyst, and further hinder the binding of soluble N₂ on these sites. Note that the neutral condition also contains some OH⁻ owing to the ionization equilibrium of water. Considering the very low solubility of N₂ in aqueous solution, the consumed OH⁻ can be continuously supplied from the shifting of water ionization equilibrium.

Supplementary Figures and Tables

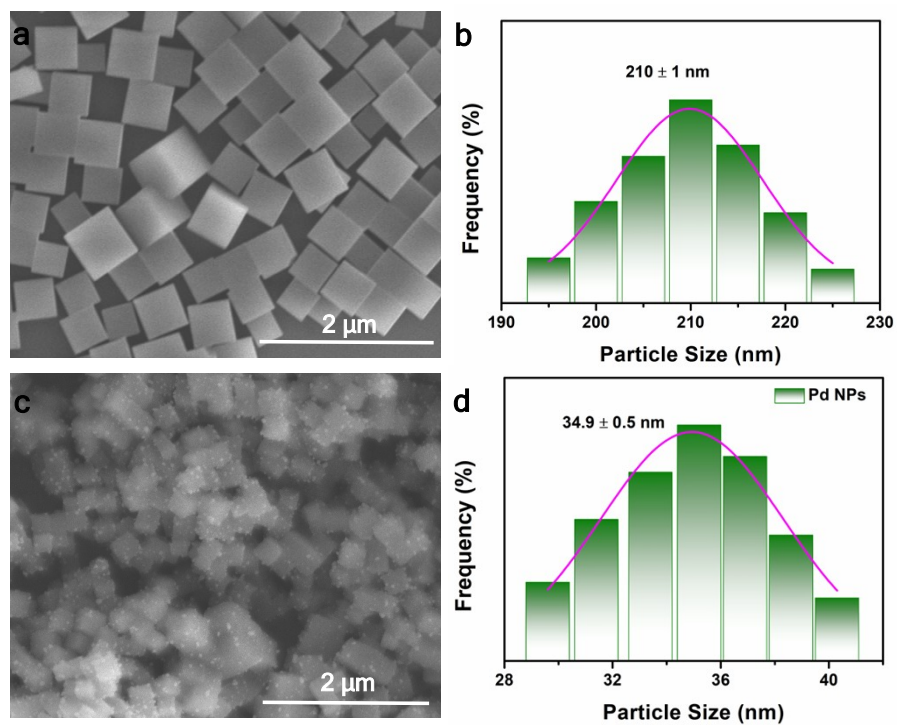


Fig. S1. SEM images and particle size histogram for PBA nanocubes and Pd/PBA nanocubes.

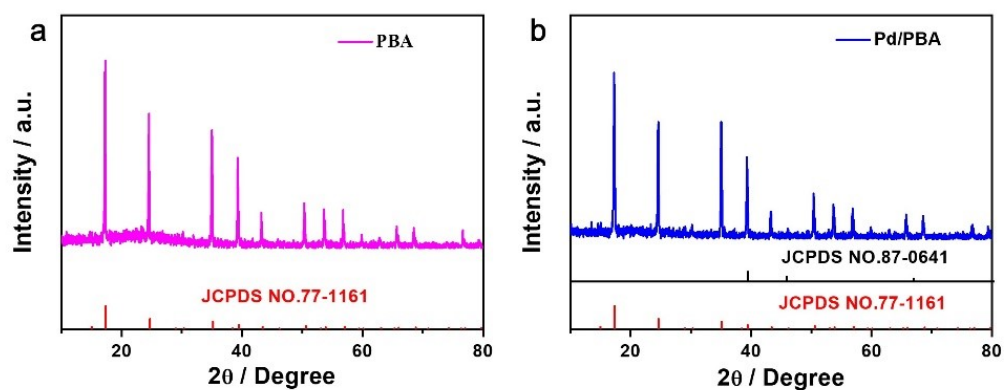


Fig. S2. XRD patterns of PBA and Pd/PBA.

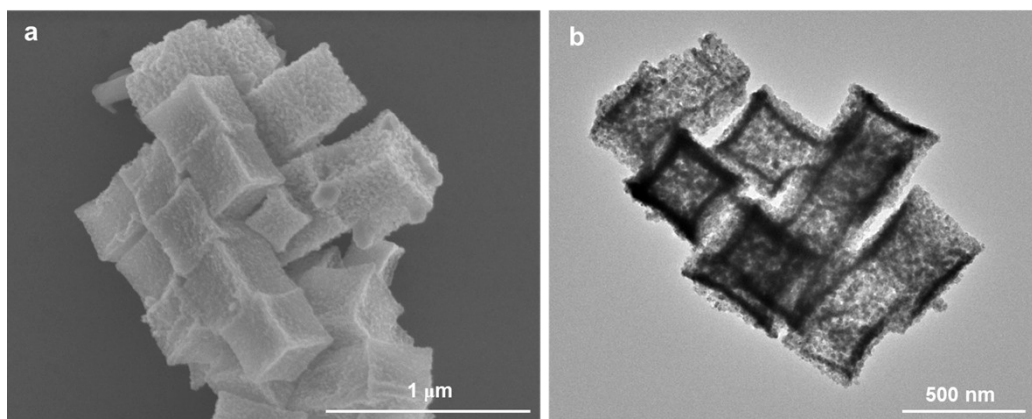


Fig. S3. (a) SEM image of the Co_3O_4 NBs. (b) TEM image of the Co_3O_4 NBs.

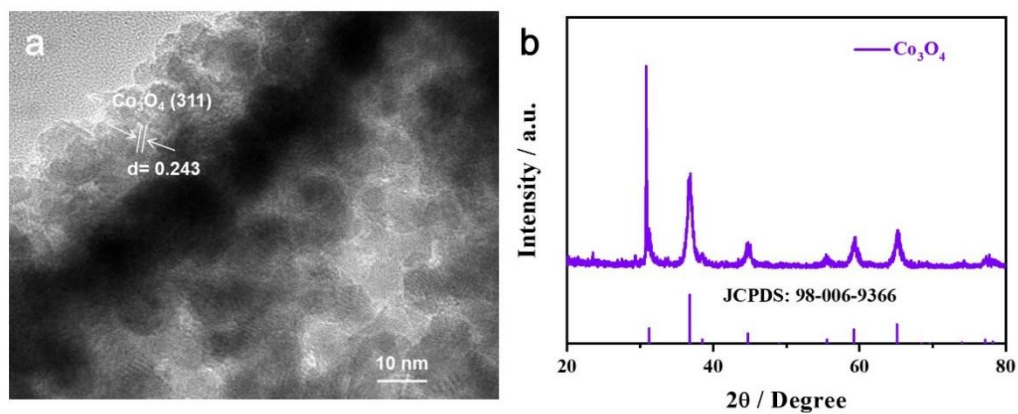


Fig. S4. (a) HRTEM image and (b) XRD pattern of the Co_3O_4 NBs.

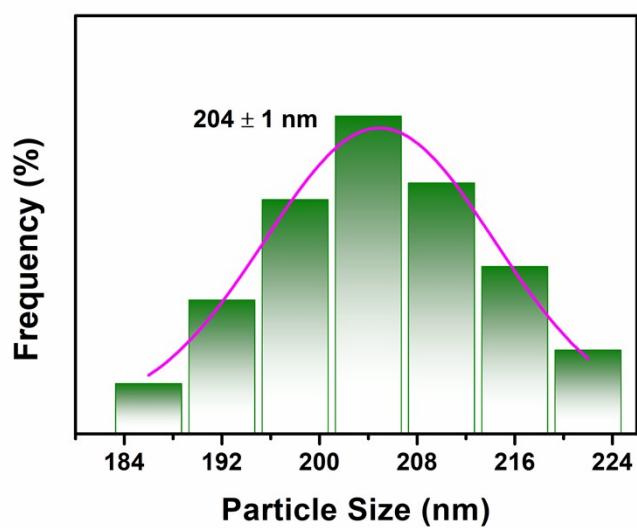


Fig. S5. Particle size histogram of the $\text{PdO}_x\text{-Co}_3\text{O}_4$ NBs.

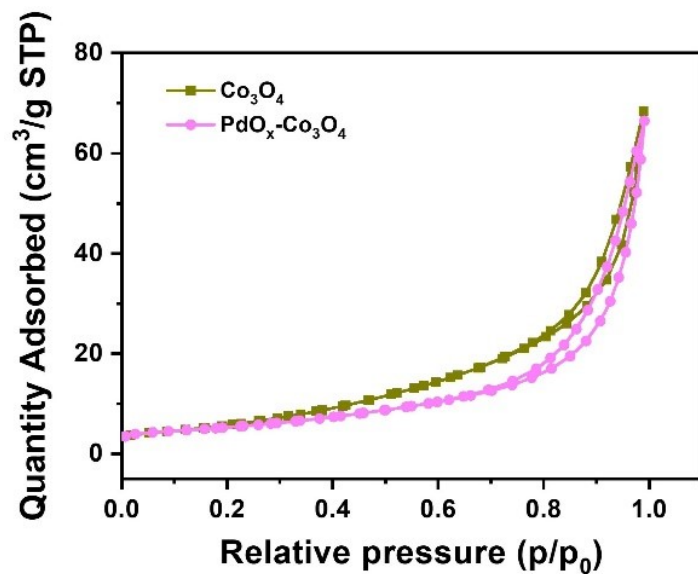


Fig. S6. N₂ adsorption and desorption isotherms of PdO_x-Co₃O₄ and Co₃O₄ NBs.

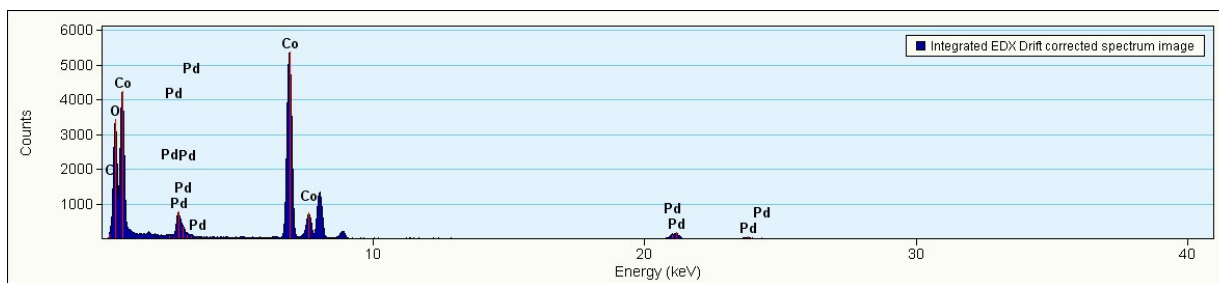


Fig. S7. TEM-EDX image of PdO_x-Co₃O₄ NBs.

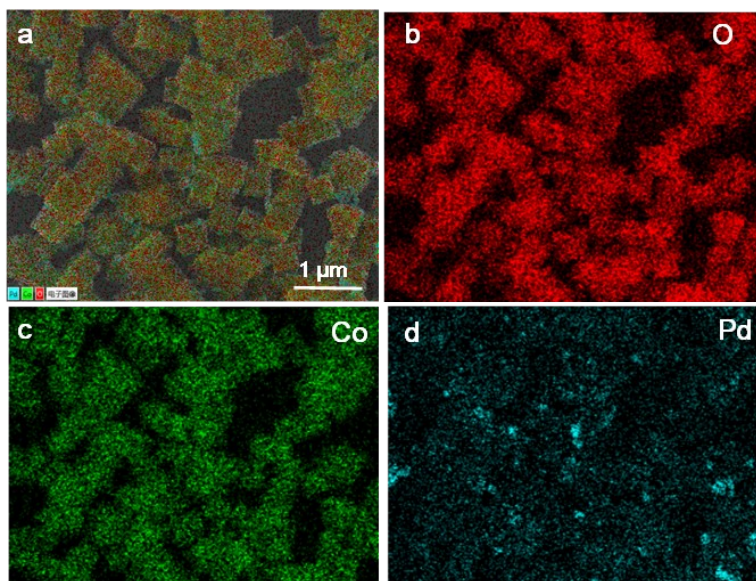


Fig. S8. SEM mapping images of PdO_x-Co₃O₄ NBs.

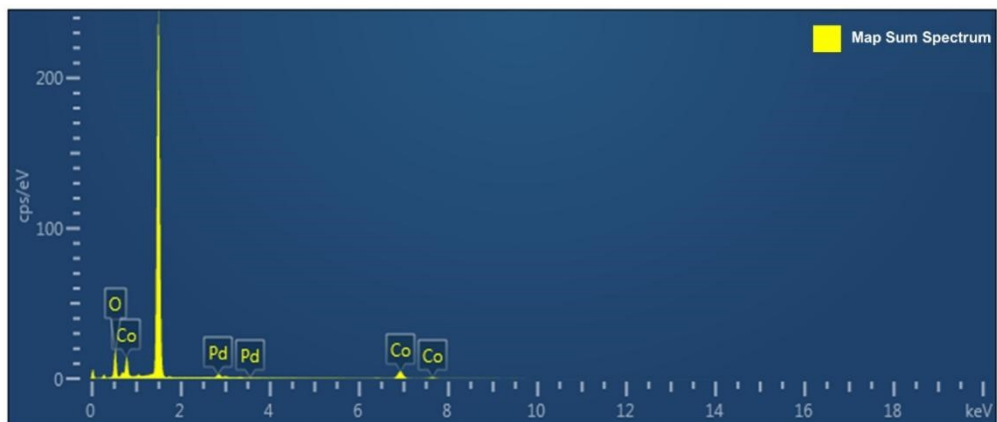


Fig. S9. SEM-EDX pattern of PdO_x-Co₃O₄ NBs.

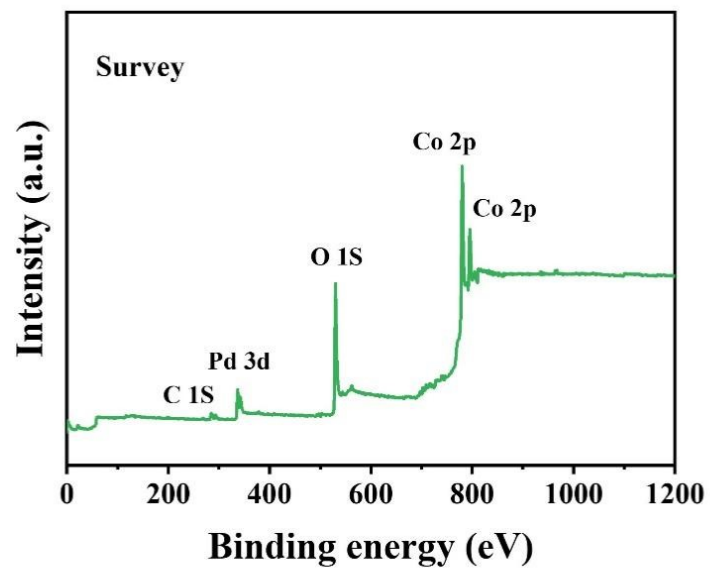


Fig. S10. XPS survey spectrum of the PdO_x-Co₃O₄ NBs.

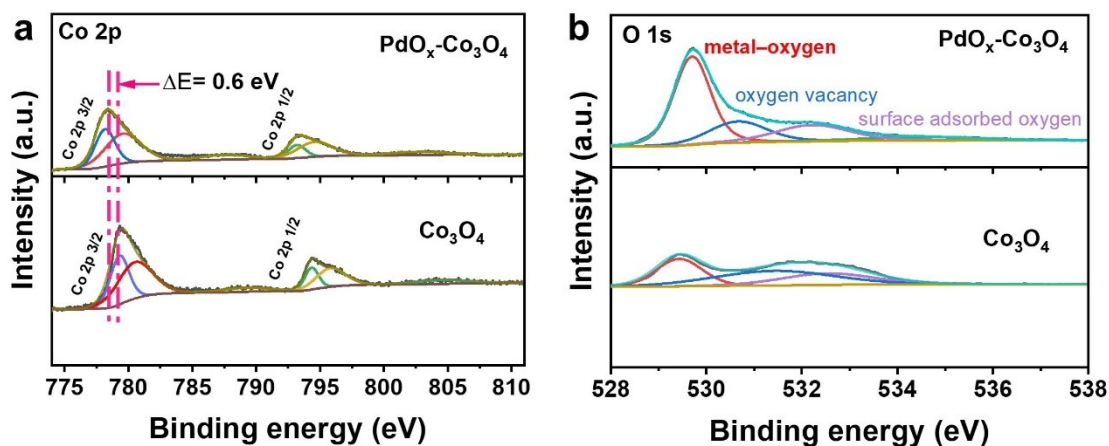


Fig. S11. XPS spectra of the PdO_x-Co₃O₄ NBs and Co₃O₄ NBs. (a) Co 2p and (b) O 1s.

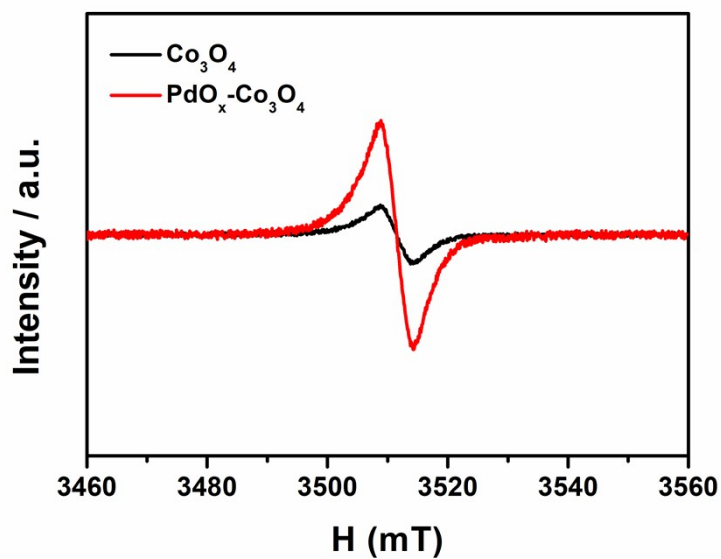


Fig. S12. EPR spectrum of the PdO_x-Co₃O₄ NBs and Co₃O₄ NBs.

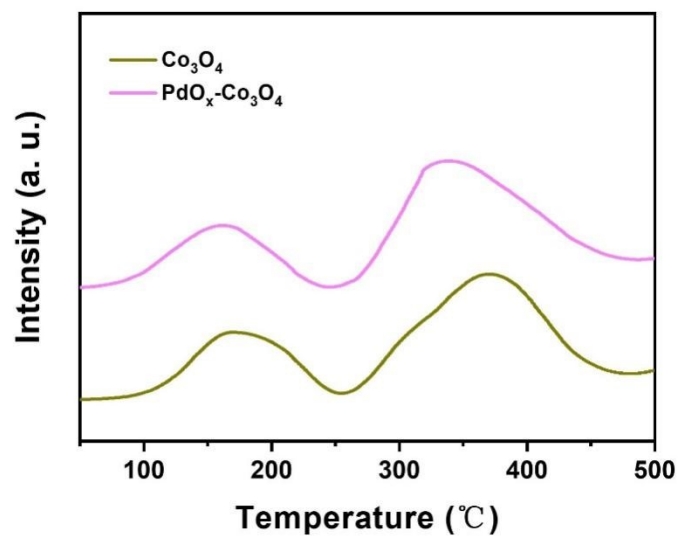


Fig. S13. N₂-TPD curves of PdO_x-Co₃O₄ and Co₃O₄.

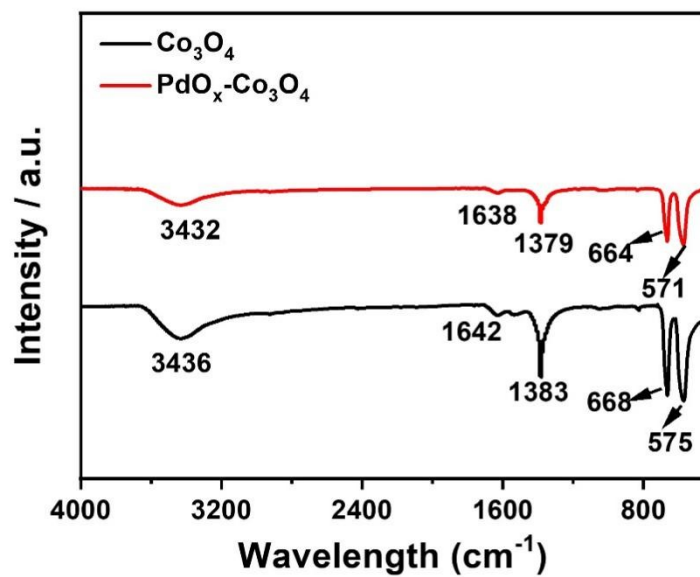


Fig. S14. FT-IR spectrum of PdO_x-Co₃O₄ and Co₃O₄.

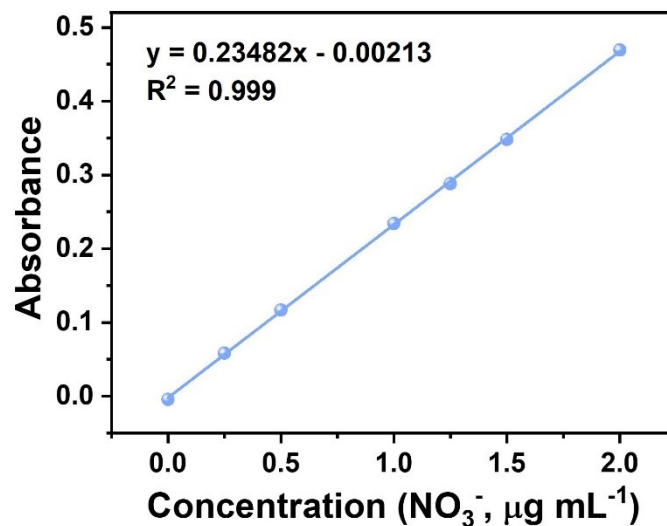


Fig. S15. The UV-Vis absorption spectra and the corresponding standard curves NO_3^- in 0.1 M Na_2SO_4 as background solution.

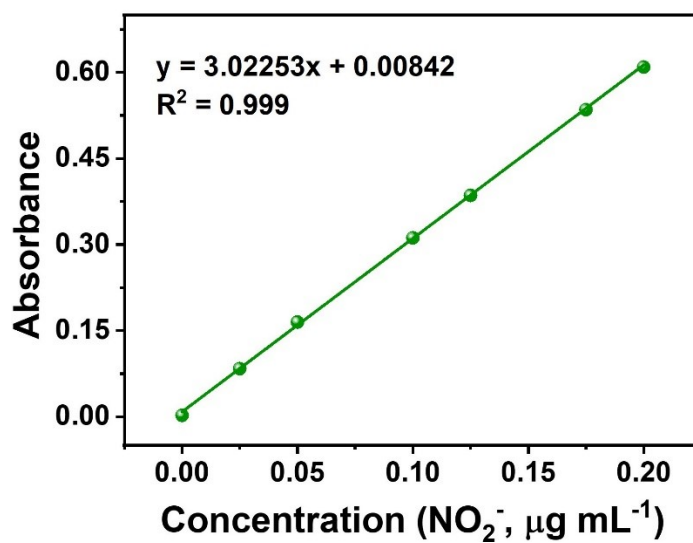


Fig. S16. The UV-Vis absorption spectra and the corresponding standard curves NO_3^- -N in 0.1 M Na_2SO_4 as background solution.

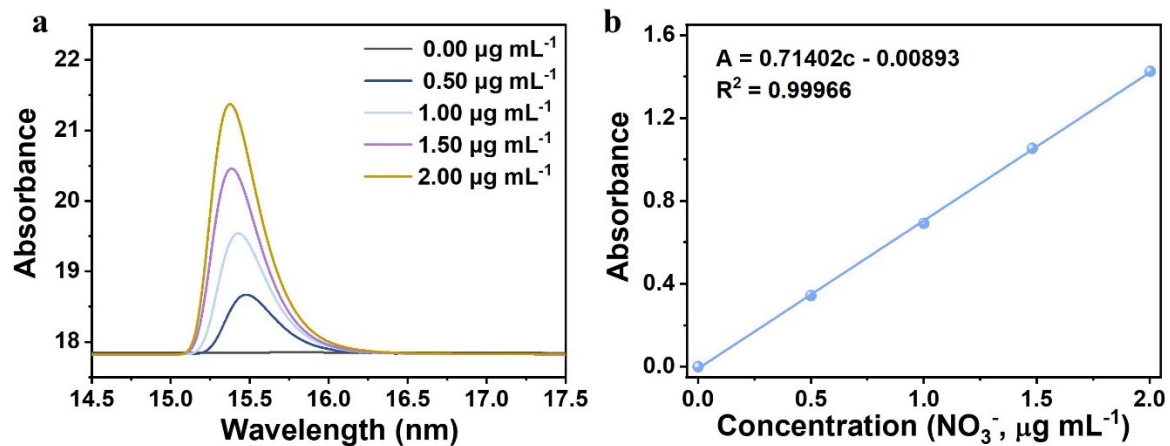


Fig. S17. NO_3^- -N quantification using IC method. (a) The IC and (b) corresponding calibration curve used for estimation of NO_3^- -N.

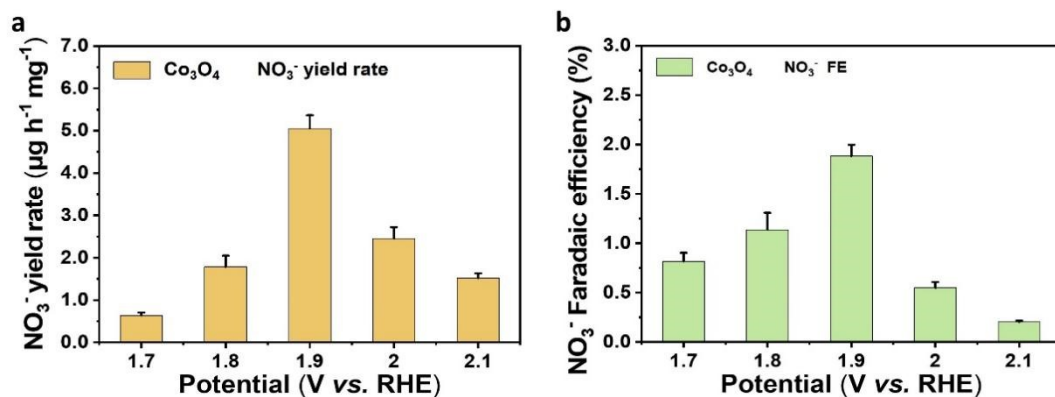


Fig. S18. NOR performance of Co_3O_4 . (a) The NO_3^- yield rate of Co_3O_4 at different potentials. (b) The FE of Co_3O_4 NBs at different potentials.

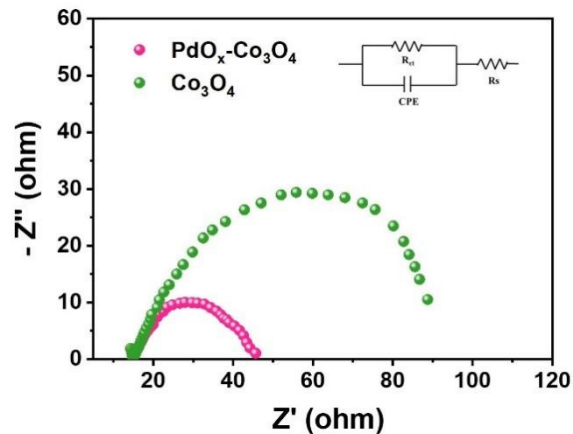


Fig. S19. Electrochemical impedance spectroscopy (EIS) of PdO_x-Co₃O₄ and Co₃O₄ NBs.

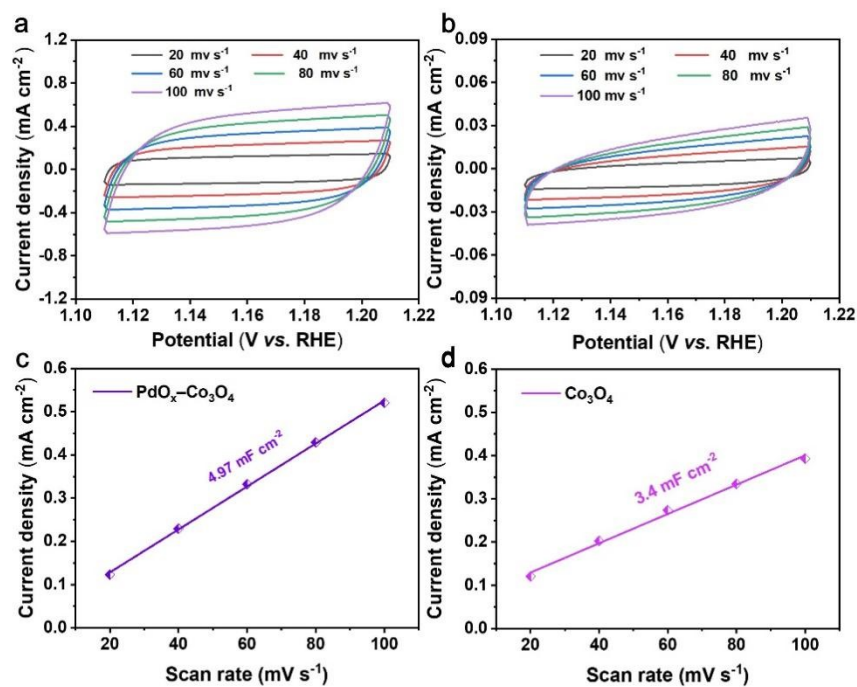


Fig. S20. Cyclic voltammograms for (a) PdO_x-Co₃O₄ NBs, (b) Co₃O₄ NBs at scan rates of 20, 40, 60, 80 and 100 mV s⁻¹. (c)-(d) The capacitive currents at 0.51 V vs. RHE as a function of scan rate for PdO_x-Co₃O₄ and Co₃O₄ NBs at scan rates of 20, 40, 60, 80 and 100 mV s⁻¹.

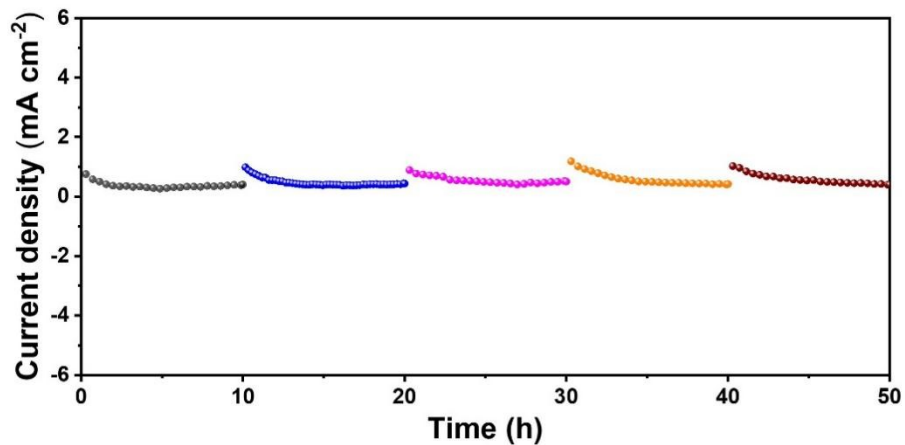


Fig. S21. Time-dependent current density curves of PdO_x-Co₃O₄ NBs with 10 h for each cycle in N₂-saturated 0.1 M Na₂SO₄ solution at 1.7 V vs. RHE.

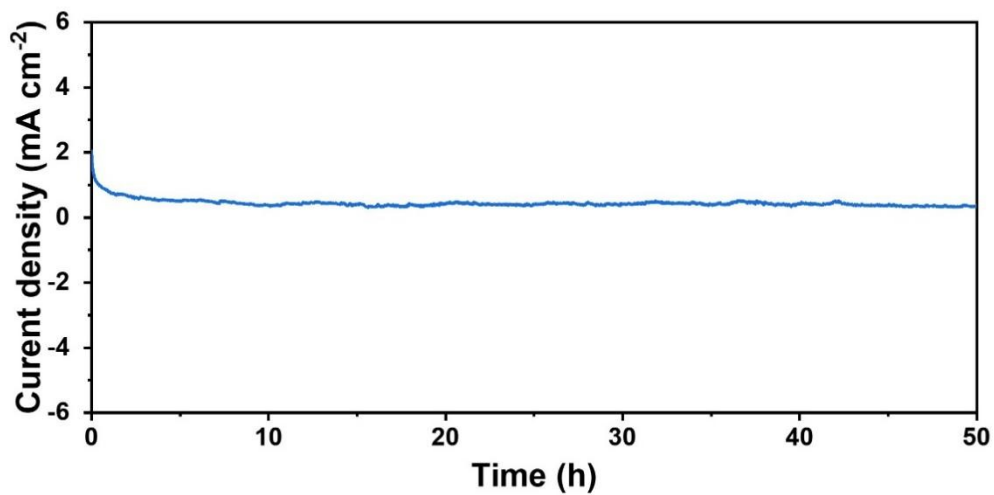


Fig. S22. The chronopotentiometric (*i*-*t*) curve for PdO_x-Co₃O₄ NBs at a potential of 1.7 V vs. RHE for 50 h.

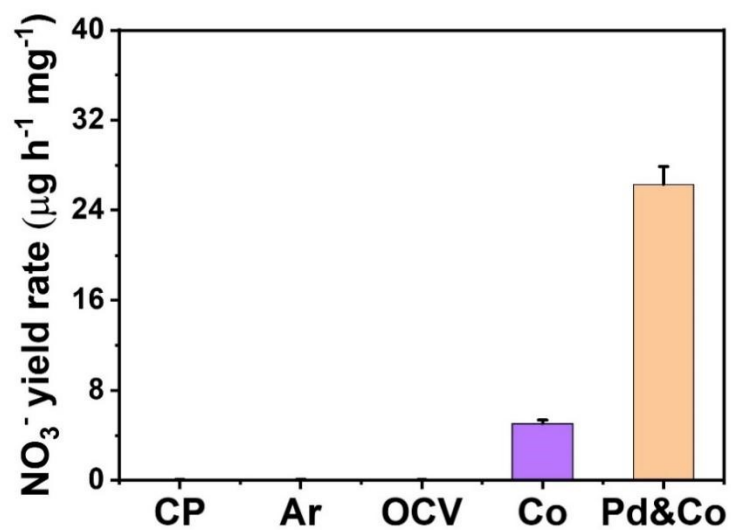


Fig. S23. UV-vis absorption spectra of 0.1 M Na_2SO_4 solution after electrolysis for 10 h in Ar-saturated and comparative study of catalysts under different operating conditions with at 1.7 V vs. RHE of $\text{PdO}_x\text{-Co}_3\text{O}_4$ NBs respectively.

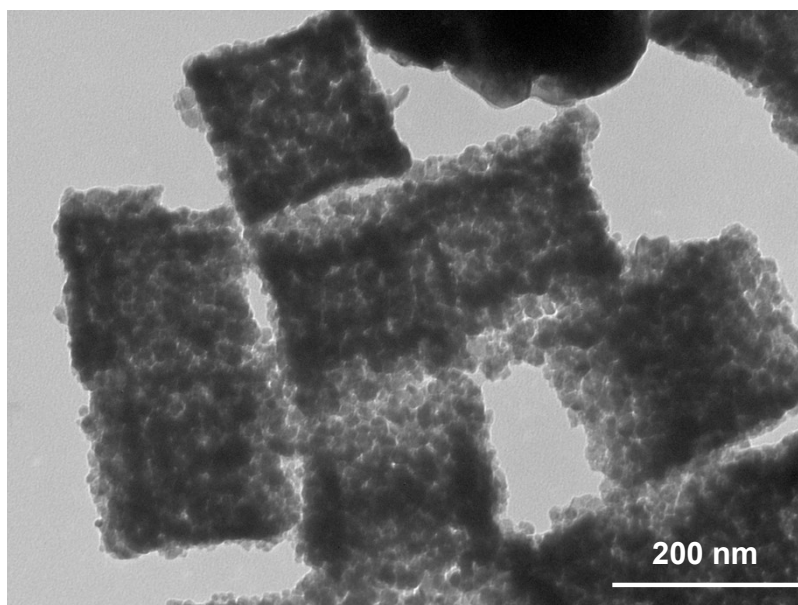


Fig. S24. The TEM image of $\text{PdO}_x\text{-Co}_3\text{O}_4$ NBs after stability test.

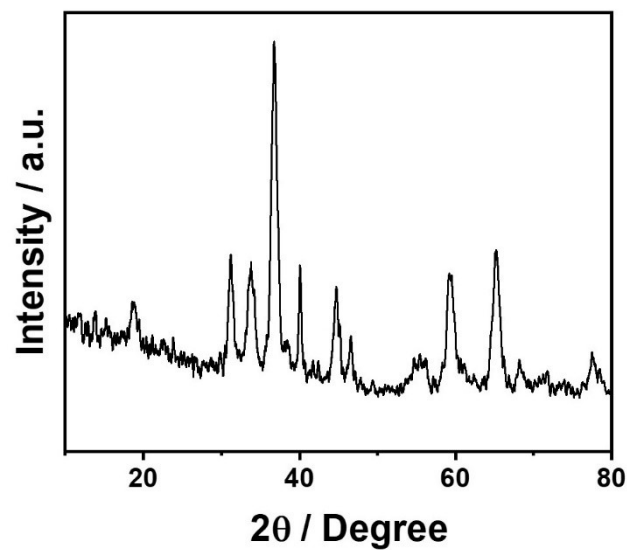


Fig. S25. XRD pattern of PdO_x-Co₃O₄ NBs after stability test.

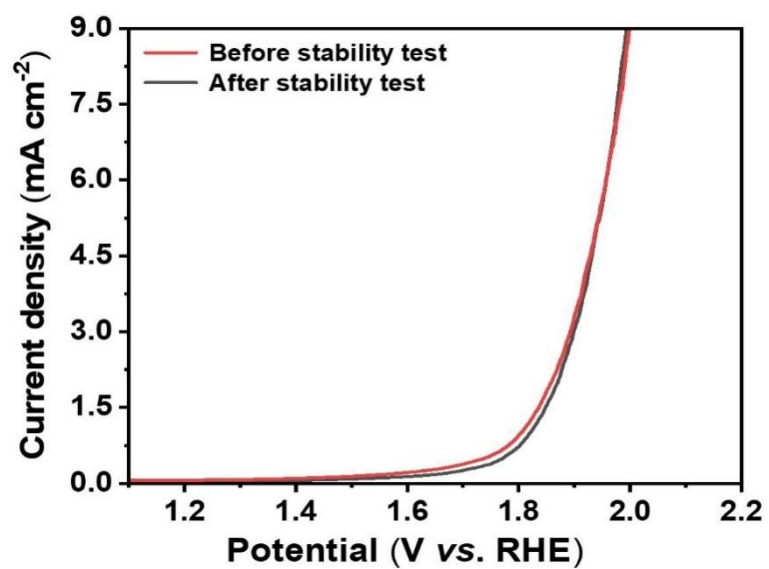


Fig. S26. LSV curves of PdO_x-Co₃O₄ NBs before and after reaction in N₂-saturated 0.1 M Na₂SO₄.

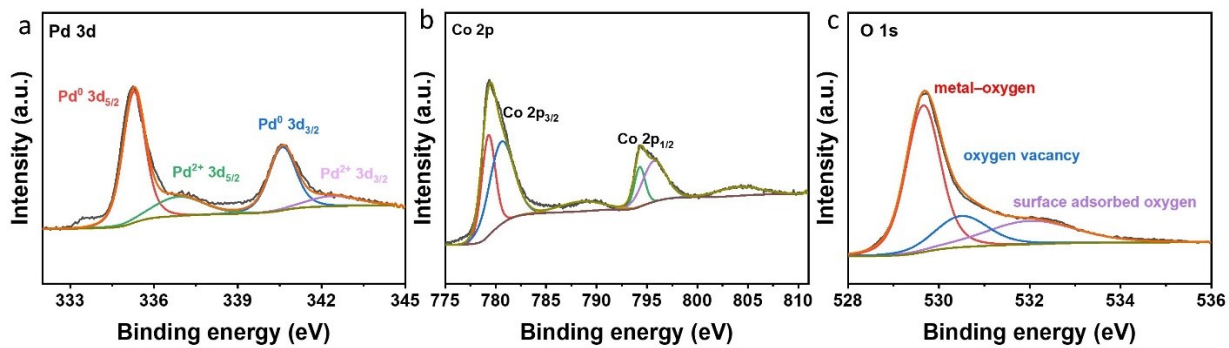


Fig. S27. XPS spectra of the PdO_x-Co₃O₄ NBs after reaction. (a) Pd 3d spectra, (b) Co 2p spectra, (c) O 1s.

Table S1. Comparison of different electrocatalysts reported in NOR at low overpotential under ambient condition.

Catalysts	Electrolyte	Yield rate $\mu\text{g h}^{-1} \text{mg}^{-1} \text{cat}$	Faradaic efficiency (%)	Ref.
PdO_x-Co₃O₄ NBs	0.1 M Na₂SO₄	26.68 (1.7 V)	5.88 (1.7 V)	This Work
TiO ₂ /RuO ₂	0.1 M Na ₂ SO ₄	10.04 (2.2 V)	26.1 (1.8 V)	^[1] Adv. Mater. 2020, 32 (26), 2002189.
Fe-SnO ₂	0.05 M H ₂ SO ₄	42.9 (1.96 V)	0.84 (1.96V)	^[2] Angew. Chem. Int. Ed. 2020, 59 (27), 10888-10893.
ZnFe _{0.4} Co _{1.6} O ₄	1 M KOH	2.1 (1.6 V)	10.1 (1.5 V)	^[3] Angew. Chem. Int. Ed. 2020, 59 (24), 9418-9422.
Pd-s PNSs	0.1 M KOH	18.56 (1.75 V)	2.5 (1.55 V)	^[4] Angew. Chem. Int. Ed. 2021, 60 (9), 4474-4478.
Pd-MXene	0.01 M Na ₂ SO ₄	2.8 (2.03 V)	11.34 (2.03 V)	^[5] Chem. Commun. 2020, 56 (43), 5779-5782.

References

- [1] M. Kuang, Y. Wang, W. Fang, H. Tan, M. Chen, J. Yao, C. Liu, J. Xu, K. Zhou, Q. Yan, *Adv. Mater.*, 2020, **32** (26), 2002189.
- [2] L. Zhang, M. Cong, X. Ding, Y. Jin, F. Xu, Y. Wang, L. Chen, L. Zhang, *Angew. Chem. Int. Ed.*, 2020, **59**, 10888-10893.
- [3] C. Dai, Y. Sun, G. Chen, A. C. Fisher, Z. Xu, *Angew. Chem. Int. Ed.*, 2020, **59**, 9418-9422.
- [4] S. Han, C. Wang, Y. Wang, Y. Yu, B. Zhang, *Angew. Chem. Int. Ed.*, 2021, **60**, 4474-4478.
- [5] W. Fang, C. Du, M. Kuang, M. Chen, W. Huang, H. Ren, J. Xu, A. Feldhoff, Q. Yan, *Chem. Commun.*, 2020, **56**, 5779-5782.